

**m**

MECSE 1996-5

**o**

**Multiple Order Laplacian Splines -  
Including Splines with Tension**

**F. Chen and D. Suter**

**n**

**a**

**July 18, 1996**

**s**

TECHNICAL REPORT  
DEPARTMENT OF ELECTRICAL AND  
COMPUTER SYSTEMS ENGINEERING,  
FACULTY OF ENGINEERING,  
MONASH UNIVERSITY, CLAYTON 3168,  
VIC, AUSTRALIA

**h**

COPYRIGHT ©1996 F. Chen and D. Suter

NOTE: This report is liable to revision.

It should not be reproduced in whole or in part without prior permission.

It may, however, be quoted as a reference.

# Multiple Order Laplacian Splines - Including Splines with Tension

F. Chen and D. Suter  
Dept. Elect. & Comp. Syst. Eng.  
Monash University  
Clayton 3168, Vic.  
Aust.

July 18, 1996

## 1 Introduction

Various authors have generalized the Laplacian spline family (of which the best known member is the thin-plate spline) to include tension. In particular [1] define what they call the  $L^{m,l,s}$ -splines (see section 2.1). However, they have not derived the explicit expressions for the kernels of such splines (nor have they given a general method for constructing such).

In this paper, we give a general method for constructing “splines with tension”. The method is based on the Fourier transform techniques. We also illustrate with some examples of interpolants using these splines.

In section 2.1, we derive the kernel functions for splines with tension and show a general method for constructing kernels for any member of the family. In general, for the space dimensions of interest 1 to 3, we find that the kernels involve combination of terms of the form  $r^k$ ,  $r^k \log r$ ,  $e^{\phi r}$  and  $K_0(\phi r)$ . Evaluation of kernels in even dimensions is discussed in section 2.2 - we discuss these in detail because such kernels involve the modified bessel function  $K_0$  as some of its terms (and this function is, perhaps, less well known, than the functions associated with other terms). In section 2.3, we demonstrate how the parameters effect the properties of kernels and make a comparison of such kernels and polyharmonic kernels. In section 3, some numerical simulations show the behavior of the interpolants constructed by different smoothness conditions. Section 4 concludes our work.

## 2 Spline with Tension

In this section we derive kernel functions for some splines in a family studied in [1][2]. In so doing, we not only derive new members of the family, but we also demonstrate a general method for deriving the kernel functions for any member of the family.

Indeed, we only need to use a couple of standard results (equation (18) [3] and equation (19) [4]) and to decompose the inverse Fourier transform of a certain PDE into partial fractions. The PDE is determined by the smoothness of the spline. For example, a well-known member of Laplacian spline family is a thin-plate spline (see Duchon [5]), which minimizes the bending energy of a thin flexible plate as it passes through the data points. The kernel function of the thin-plate spline is a Green's function for the 2-iterated Laplacian and the associated PDE is  $\Delta^2 K = \delta$ . The thin-plate spline interpolant involves the linear combination of  $r^2 \log r$  kernel. In following subsection 2.1, we discuss more complex situations, in which the smoothness conditions will be decomposed into multiple terms.

### 2.1 Kernel Functions

#### 2.1.1 Thin-plate spline with tension

Consider the smoothness functional, formed from a first order and second order Laplacian operator, associated with the PDE  $(-\phi^2 \Delta + \Delta^2)K = \delta$ , where tension parameter  $\phi$  controls the amount of first order smoothness. We wish to calculate the inverse Fourier transform of:

$$\frac{1}{\phi^2 q^2 + q^4} = \frac{1}{\phi^2} \left( \frac{1}{q^2} - \frac{1}{\phi^2 + q^2} \right) \quad (1)$$

For the first part, we can use equation (18) ( Appendix B) and for the latter part we can use equation (19) (Appendix C). We will simply give the expressions for the kernel in low dimensions:

- For  $n = 1$  we have:

$$K(r) = -\frac{1}{2\phi^2} \left( r + \frac{e^{-\phi r}}{\phi} \right) \quad (2)$$

- For  $n = 2$  we have:

$$K(r) = -\frac{1}{2\pi\phi^2} (\log r + K_0(\phi r)) \quad (3)$$

#### 2.1.2 Second and third order Laplacian spline

We can also have a smoothness functional with second and third orders smoothness terms. The associated PDE is  $(\Delta^2 - \tau^2 \Delta^3)K = \delta$ , and parameter  $\tau$  controls the amount

of third order smoothness. We wish to calculate the inverse Fourier transform of:

$$\frac{1}{q^4 + \tau^2 q^6} = \frac{-\tau^2}{q^2} + \frac{1}{q^4} + \frac{\tau^2}{\frac{1}{\tau^2} + q^2} \quad (4)$$

For the first and second parts, we can use equation (18) and for the latter part we can use equation (19). We will simply give the expressions for the kernel in low dimensions:

- For  $n = 1$  we have:

$$K = \frac{\tau^2 r}{2} + \frac{r^3}{12} + \frac{\tau^3}{2} e^{\frac{-r}{\tau}} \quad (5)$$

- For  $n = 2$  we have:

$$K = \frac{1}{2\pi} (\tau^2 \log r + \frac{r^2}{4} \log r + \tau^2 K_0(\frac{r}{\tau})) \quad (6)$$

- For  $n = 3$  we have:

$$K = \frac{\tau^2}{4\pi r} (-1 - \frac{r^2}{2\tau^2} + e^{\frac{-r}{\tau}}) \quad (7)$$

### 2.1.3 First, second and third order Laplacian spline

Now consider the smoothness functional, formed from a first, second and third order smoothness terms. The associated PDE is  $(-\phi^2 \Delta + \Delta^2 - \tau^2 \Delta^3)K = \delta$ , where  $\tau$  and  $\phi$  are two parameters controlling the first order term and the third order term, respectively. We wish to calculate the inverse Fourier transform of:

$$\frac{1}{\phi^2 q^2 + q^4 + \tau^2 q^6} = \frac{1}{\phi^2} \left( \frac{1}{q^2} + \frac{-\tau^2 q^2 - 1}{\phi^2 + q^2 + \tau^2 q^4} \right) \quad (8)$$

For the first term in brackets, we can use equation (18) and for the latter part, consider the general problem:

$$\mathcal{F}^{-1} \left( \frac{Aq^2 + B}{c + bq^2 + dq^4} \right) = \mathcal{F}^{-1} \left( \frac{1}{d} \left( \frac{C}{(q^2 + w)} + \frac{D}{(q^2 + v)} \right) \right) \quad (9)$$

where

$$v = \frac{b + \sqrt{b^2 - 4cd}}{2d}, \quad w = \frac{b - \sqrt{b^2 - 4cd}}{2d}, \quad C = \frac{B - Aw}{v - w}, \quad D = \frac{Av - B}{v - w}$$

One can now use equation (19) on the two parts of the above decomposition. Again, we obtain the relative expressions for low dimensions:

- For  $n = 1$  we have:

$$K(r) = \frac{1}{\phi^2} \left( -\frac{r}{2} + \frac{1}{2(v-w)} \left( \frac{w}{\sqrt{v}} e^{-\sqrt{v}r} - \frac{v}{\sqrt{w}} e^{-\sqrt{w}r} \right) \right) \quad (10)$$

- For  $n = 2$  we have:

$$K(r) = \frac{1}{2\pi\phi^2}(-\log r + \frac{1}{(v-w)}(wK_0(\sqrt{v}r) - vK_0(\sqrt{w}r))) \quad (11)$$

- For  $n = 3$  we have:

$$K(r) = \frac{1}{4\pi r\phi^2}(1 + \frac{1}{v-w}(we^{-\sqrt{v}r} - ve^{-\sqrt{w}r})) \quad (12)$$

Here,

$$v = \frac{1 + \sqrt{1 - 4\tau^2\phi^2}}{2\tau^2}, \quad w = \frac{1 - \sqrt{1 - 4\tau^2\phi^2}}{2\tau^2}$$

are two roots of the quadratic equation  $\tau^2q^4 + q^2 + \phi^2 = 0$ .

It is obvious that when the discriminant  $1 - 4\tau^2\phi^2 \geq 0$ ,  $v$  and  $w$  are two real roots. The kernel functions are real functions. As we now show, the same holds if  $1 - 4\tau^2\phi^2 < 0$ . When  $1 - 4\tau^2\phi^2 < 0$ ,  $v$  and  $w$  are a pair of conjugate complex roots. In even dimensions, the kernels involve the modified Bessel function  $K_0$ . From the expression (14) of  $K_0$  (see section 2.2), it can be seen that the modified bessel function  $K_0$  has the property: if  $x = \bar{y}$ , then  $K_0(x) = \overline{K_0(y)}$ . Hence, for the kernel (11) in two dimensions, when  $1 - 4\tau^2\phi^2 < 0$ ,  $v = \bar{w}$ ,  $\sqrt{v} = \overline{\sqrt{w}}$ , and the expression  $(wK_0(\sqrt{v}r) - vK_0(\sqrt{w}r))$  is pure imaginary, which is divided by another pure imaginary  $(v-w)$ . Thus, the kernel function  $K(r)$  is still a real function. It is easy to deduce the same conclusion for odd dimensions, in which the kernel involves in exponential function.

#### 2.1.4 Other members of multiple order Laplacian splines

For the vector splines in 3D we will need the (scalar) kernel associated with the PDE  $(\Delta + \tau^2\Delta^3) = \delta$ . This is essentially because we need the first order smoothness to ensure the null space contains only constants, and we also need the third order to ensure the spline is smooth enough (particularly at the data points). We will also need the (scalar) kernel associated with the PDE  $(\Delta^2 + \tau^2\Delta^4)K = \delta$ . This is because the vector spline is defined in terms of the derivatives of the kernel that is one order higher than the scalar spline (to which it reduces on some combinations of parameters). In appendix D, we will derive the kernels for these two models.

For any member of this family, the kernel functions can be obtained by the decomposition of the fractional expression into the partial ones and then by using inverse Fourier transform similar to those used in the above examples. A number of kernel functions associated with different smoothness functionals will be listed in Table 1 (appendix A).

## 2.2 Evaluation of Kernels

The expressions for the kernels we have derived will involve (in even dimensions) the modified Bessel function  $K_0$ . In order to evaluate such kernels, we need to find ways of evaluating these Bessel functions *in combination* with other terms with a logarithmic divergence at the origin. Here, we explain with an example, how this is done.

For example, in two dimensions, the kernel function of thin-plate spline with tension has the expression:

$$K(r) = -\frac{1}{2\pi\phi^2}[\log r + K_0(r\phi)], \quad (13)$$

where  $K_0$  is the zero order modified bessel function of the second kind.

The modified bessel function  $K_0$  has power series form (see [6], pp375):

$$K_0(z) = (\log 2 - c_E)I_0(z) - I_0(z) \log z + \sum_{k=1}^{\infty} \left(1 + \frac{1}{2} + \dots + \frac{1}{k}\right) \frac{\left(\frac{1}{4}z^2\right)^k}{(k!)^2} \quad (14)$$

where  $c_E$  is Euler's constant,  $I_0(z)$  is the zero order modified bessel function of the first kind, and

$$I_0(z) = \sum_{k=0}^{\infty} \frac{\left(\frac{1}{4}z^2\right)^k}{(k!)^2}$$

For large  $z$ , the asymptotic expansion of  $K_0$  is (see [6], pp378):

$$K_0(z) = \left(\frac{\pi}{2z}\right)^{\frac{1}{2}} e^{-z} \left(1 - \frac{1}{8z} + \frac{1^2 \cdot 3^2}{2!} \frac{1}{(8z)^2} - \frac{1^2 \cdot 3^2 \cdot 5^2}{3!} \frac{1}{(8z)^3} + \dots\right) \quad (15)$$

Figure 1 depicts the modified bessel functions  $K_0$  and  $I_0$  in one dimension, respectively.

Now we analyse the limit properties of the kernel function  $K(r)$  in (13). When  $r \rightarrow 0$ , from (14),  $I_0(r) \rightarrow 1$ , and

$$K_0(\phi r) \rightarrow \log \frac{2}{\phi} - c_E - \log r \rightarrow \infty$$

and when  $r \rightarrow \infty$ , from (15)

$$K_0(\phi r) \rightarrow 0$$

Hence, we have

$$\lim_{r \rightarrow 0} K(r) = -\frac{1}{2\pi\phi^2} \left(\log \frac{2}{\phi} - c_E\right),$$

and

$$\lim_{r \rightarrow \infty} K(r) = \lim_{r \rightarrow \infty} -\frac{1}{2\pi\phi^2} \log r = -\infty$$

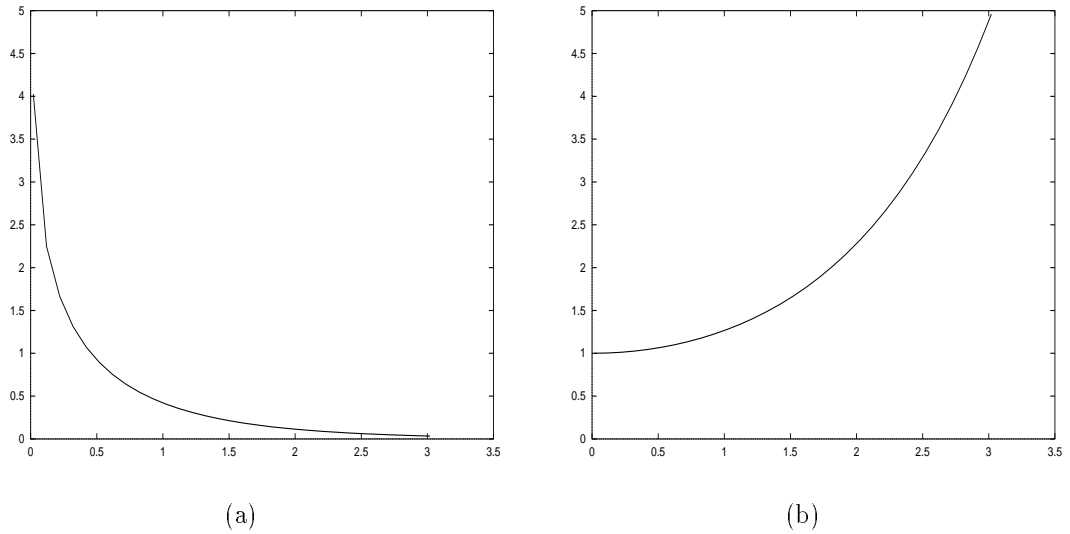


Figure 1: Graphs of modified Bessel function  $K_0$  and  $I_0$ . (a) second kind modified Bessel function  $K_0$ . (b) first kind modified Bessel function  $I_0$ .

It can be seen that the modified Bessel function  $K_0$  is difficult to evaluate because it diverges at the origin, but in combination with a logarithmic function which also diverges at the origin, the singularity is removed. Hence, the kernel function converges to a constant at the origin. In addition, the kernel can be approximated by a logarithmic function at infinity. The similar properties can be derived for other members of Laplacian spline family in even dimensions.

For odd dimensions, it is much easier to evaluate kernel function since such kernels are a combination of the exponential functions and a polynomial.

### 2.3 Properties of kernels

Several parameters play an important role in multiple order Laplacian spline models. They influence the properties of kernels. In this subsection, we will discuss how multiple order Laplacian kernels change their form with changes in parameters, and present a comparison of these kernels with polyharmonic kernels (or harmonic kernels).

For example, consider the thin-plate spline with tension model  $(-\phi^2\Delta + \Delta^2)K = \delta$ . When tension parameter  $\phi$  becomes more and more large, the model is dominated by the first order term, hence the corresponding kernels tend to first order kernel. Otherwise, when  $\phi$  becomes more and more small, the model is second order term dominated: the kernel tends to the second order thin-plate spline kernel. Figure 2 illustrate the behaviour of the kernels changing with different parameters.

Figure 2 (a) shows the kernel function (3) of first and second order Laplacian spline

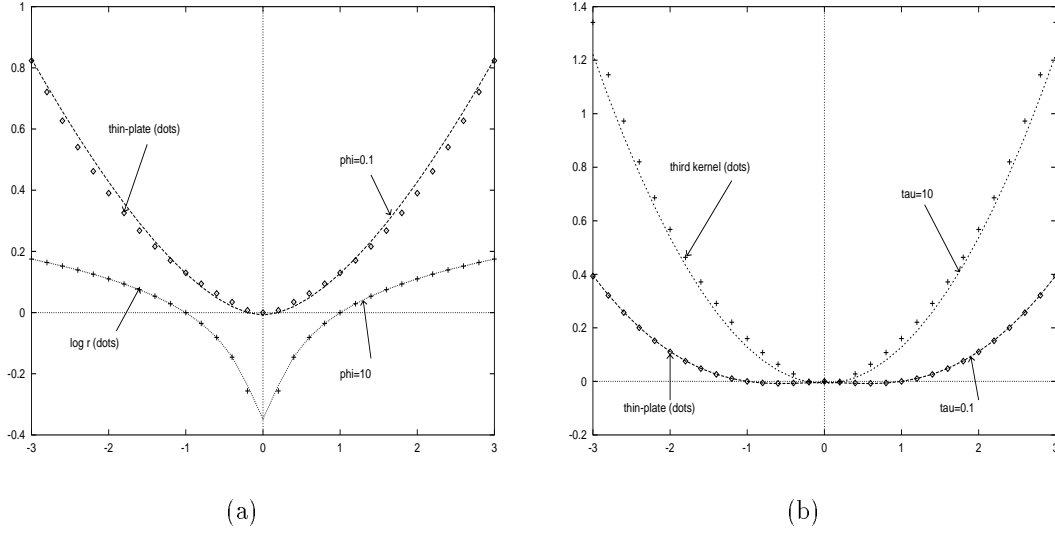


Figure 2: Graphs of  $L^{m,l,s}$  kernels with different parameters. (a) plot of the kernels of the first and second order Laplacian spline with the parameters  $\phi = 10$  and  $\phi = 0.1$ , and a comparison of these kernels with the first order kernel  $\log r$  (dotted line) and the thin-plate kernel (dotted line). (b) plot of the kernels of the second and third order Laplacian spline with the parameters  $\tau = 10$  and  $\tau = 0.1$ , and a comparison of these kernels with the thin-plate spline kernel (dotted line) and the third order Laplacian kernel (dotted line).

changing with different tension parameter  $\phi$  (here, we plot the negative of the kernel for comparison with first order kernel and second order thin-plate spline kernel, it does not change the properties of the kernels). It can be seen that when  $\phi$  becomes smaller (in figure,  $\phi = 0.1$ ), the kernel function is very close to the thin-plate spline kernel (plotted in dotted line), - here we use the kernel  $r^2 \log r / 8\pi + 0.15r - 0.02$  rather than the standard biharmonic (thin-plate spline) kernel  $r^2 \log r / 8\pi$  for comparison purpose, because the linear term and constant can be absorbed into the null space. Conversely, when  $\phi$  becomes bigger (in figure,  $\phi = 10$ ), the kernel function is very close to the harmonic (membrane) kernel  $\log r$  (plotted in dotted line).

Figure 2 (b) shows the kernel (6) of second and third order Laplacian spline with different parameter  $\tau$ . When  $\tau$  becomes smaller (in figure,  $\tau = 0.1$ ), the kernel is very close to the thin-plate spline kernel (plotted in dotted line). Otherwise, when  $\tau$  becomes bigger (in figure,  $\tau = 10$ ), the kernel tend to the triharmonic kernel (plotted in dotted line) - again, we use the kernel  $r^4 \log r / 128\pi + 0.1r^2 + 0.08r - 0.02$  rather than the standard triharmonic kernel  $r^4 \log r / 128\pi$  for comparison purpose, because the null space of the third order Laplacian spline is a quadratic polynomial.

In conclusion, the properties of kernels of multiple order Laplacian spline depend on the parameters. By choosing the limits as these parameters tend either to 0 or to  $\infty$ , we



can establish a connection between multiple Laplacian kernels and polyharmonic kernels.

### 3 Examples of Interpolants

In this section, some numerical examples on reconstructing an interpolation surface from scattered data are given using different smoothness constraints.

For given  $N$  scattered data points  $X_i = (x_i, y_i, z_i)$ ,  $i = 1, \dots, N$  in  $R^3$ , we interpolate values of  $z$  to form a smooth surface  $z(x, y)$  by using multiple order Laplacian splines. The interpolant is given by:

$$s(X) = \sum_{i=1}^N c_i K(|X - X_i|) + p_M(X) \quad (16)$$

where  $K(X)$  is the kernel functions associated with a smoothness constraint,  $c_i$  ( $i = 1, \dots, N$ ) are coefficients.  $p_M(X) \in P_M$  (all polynomials of degree less than or equal to  $M$ ) and  $M$  denotes the dimension of the null space. In multiple order Laplacian spline models, the dimension of the null space depends on the lowest order Laplacian operator in the PDE.  $M = \binom{n+m-1}{n}$ , here,  $m$  is the order of the lowest order of Laplacian operator in the PDE.

The coefficients  $c_i$  and  $p_M$  are determined by following equations:

$$\begin{aligned} s(X_i) &= z_i \\ \sum_{i=1}^N c_i q(X_i) &= 0 \end{aligned} \quad (17)$$

where  $q(X) \in P_M$ .

Figures 3 through 6 are all reconstructions from the same sample points. We use Gu's *rkpk* package [7] for solving the linear system (17). The data set consists of 25 points given as follows:

$$\begin{array}{ccccc} (-1, -1, 1) & (-1, -.5, 1) & (-1, 0, 1) & (-1, .5, 1) & (-1, 1, 1) \\ (-.5, -1, 1) & (-.5, -.5, 2) & (-.5, 0, 2) & (-.5, .5, 2) & (-.5, 1, 1) \\ (0, -1, 1) & (0, -.5, 2) & (0, 0, 3) & (0, .5, 2) & (0, 1, 1) \\ (.5, -1, 1) & (.5, -.5, 2) & (.5, 0, 2) & (.5, .5, 2) & (.5, 1, 1) \\ (1, -1, 1) & (1, -.5, 2) & (1, 0, 2) & (1, .5, 2) & (1, 1, 1) \end{array}$$

where  $(x, y, z)$  denotes a point in 3D coordinate system.

Figure 3 shows the interpolants using thin-plate spline with tension model  $(-\phi^2 \Delta + \Delta^2)K = \delta$ . The kernel function is given in (3). The null space is a constant. The

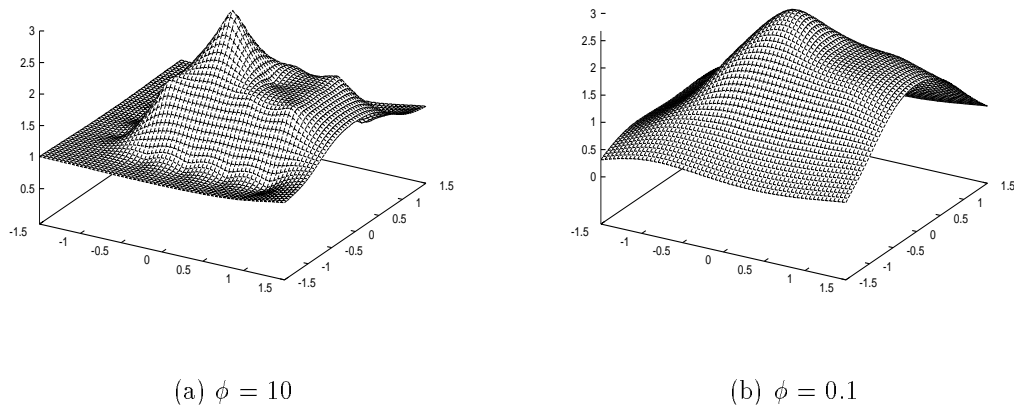


Figure 3: Interpolants with different parameter  $\phi$  using thin-plate spline with tension model  $(-\phi^2\Delta + \Delta^2)K = \delta$ . (a) shows the interpolant with a bigger  $\phi = 10$ , the surface has less smoothness. (b) shows a more smooth interpolant with a smaller parameter  $\phi = 0.1$ , the surface is close to a second order thin-plate spline interpolant (plotted in Figure 6 (a))

parameter  $\phi$  controls the relative weights on two parts. When  $\phi$  is large, the model is first order (membrane) dominated, otherwise the model close to second order thin-plate spline. (a) shows the interpolant with a larger  $\phi = 10$ . As can be seen, the surface has less smoothness. Figure 3 (b) shows a more smooth interpolant with small parameter  $\phi = 0.1$ .

Figure 4 shows the interpolants using first, second and third order Laplacian spline  $(-\phi^2\Delta + \Delta^2 - \tau^2\Delta^3)K = \delta$ . The kernel function is given in (11). The null space is a constant. There are two parameters  $\phi$  and  $\tau$  to control the relative weights on the first order term and third order term, respectively. When the tension parameter  $\phi$  becomes bigger, the model is the first order dominated and the interpolant has less smoothness, otherwise, the interpolant becomes more smooth. Similarly, when the third order parameter  $\tau$  becomes bigger, the model is dominated by the third order term, the interpolant has the third order smoothness, otherwise, the model is dominated by other two terms. When two parameters are both smaller, the model is dominated by the second order term. (a) shows the interpolant with  $\phi = 10$ ,  $\tau = 0.01$ , the surface is close to first order interpolant. (b) shows the interpolant with two small parameters  $\phi = 0.01$ ,  $\tau = 0.01$ , the interpolant is close to the thin-plate spline interpolant (see Figure 6 (a)). (c) shows the interpolant with  $\phi = 0.01$ ,  $\tau = 10$ , the surface is close to the third order interpolant (see Figure 6 (b)).

Figure 5 shows the interpolants using the second and third order Laplacian spline

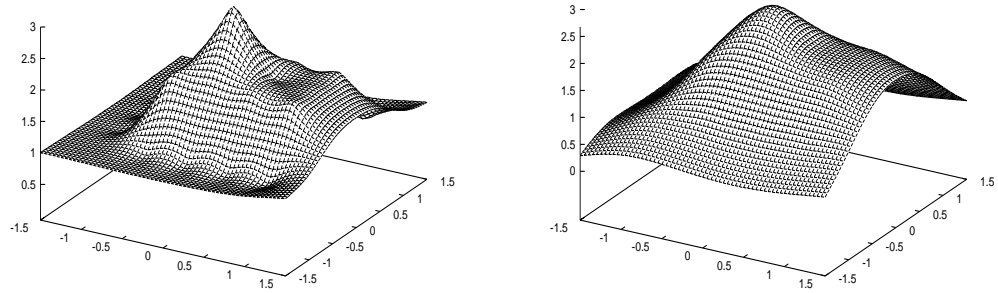
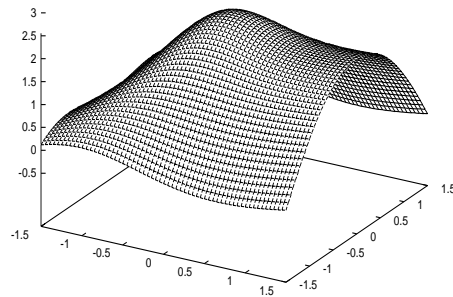
(a)  $\phi = 10, \tau = 0.01$ (b)  $\phi = 0.01, \tau = 0.01$ (c)  $\phi = 0.01, \tau = 10$ 

Figure 4: Interpolants with different parameters  $\phi$  and  $\tau$  using first, second and third order Laplacian spline  $(-\phi^2\Delta + \Delta^2 - \tau^2\Delta^3)K = \delta$ . (a) shows the interpolant with  $\phi = 10, \tau = 0.01$ , the surface is close to first order interpolant. (b) shows the interpolant with two small parameters  $\phi = 0.01, \tau = 0.01$ , the interpolant is close to the thin-plate spline interpolant (see Figure 6 (a)). (c) shows the interpolant with  $\phi = 0.01, \tau = 10$ , the surface is close to the third order interpolant (see Figure 6 (b)).

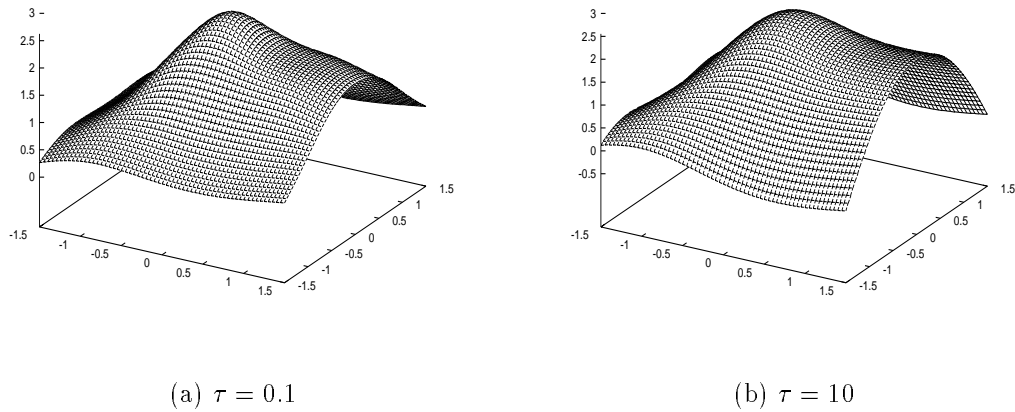


Figure 5: Interpolants with different parameter  $\tau$  using the second and third order Laplacian spline  $(\Delta^2 - \tau^2 \Delta^3)K = \delta$ . (a) shows the interpolant with  $\tau = 0.1$ , the surface is close to the thin-plate spline interpolant (see Figure 6 (a)). (b) shows the interpolant with  $\tau = 10$ , the interpolant has similar behaviour with the third order Laplacian spline interpolant (see Figure 6 (b)).

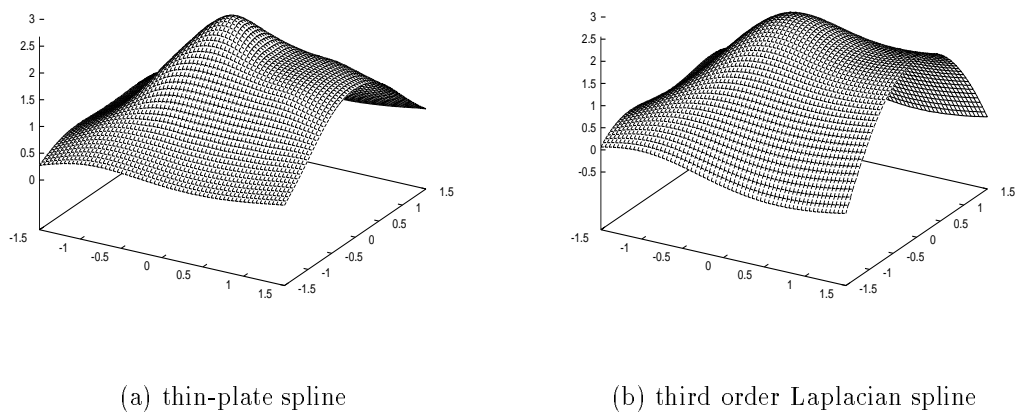


Figure 6: Interpolants using thin-plate spline and third order Laplacian spline for comparison with multiple order Laplacian interpolants

model  $(\Delta^2 - \tau^2 \Delta^3)K = \delta$ . The kernel function is given in (6). The null space is a linear polynomial. (a) shows the interpolant with a small parameter  $\tau = 0.1$ , the surface is close to the thin-plate spline interpolant (see Figure 6 (a)). (b) shows the interpolant with a large  $\tau = 10$ , the interpolant has similar behaviour with the third order Laplacian spline interpolant (see Figure 6 (b)).

Figure 6 shows the thin-plate spline interpolant and the third order Laplacian spline interpolant. The null space of the thin-plate spline is a linear polynomial, while the null space of the third order spline is a quadratic polynomial.

## 4 Summary

In this report, we have presented a general method for deriving the kernel functions of multiple order Laplacian spline. We have also discussed the properties of kernels and demonstrated the behaviour of the kernels changing with different parameters. Evaluation of kernels in even dimensions has been discussed because such kernels involve the modified Bessel function  $K_0$ .

The Laplacian spline family has advantage of controlling smoothness of interpolant by weighting differently the smoothness imposed on each part. These weight parameters make the spline model much flexible and easily to adjust to suit interpolation of different data phenomenon. In section 3, we have illustrated some examples of how the interpolants vary with the parameters.

## Appendix:

### A Table 1

The following table shows a list of kernel functions with different smoothness in low dimensions.

Smoothness	PDE	Kernel
1st+2nd	$(-\phi^2\Delta + \Delta^2)K = \delta$	n=1, $K = -\frac{1}{2\phi^2}(r + \frac{e^{-r\phi}}{\phi})$
		n=2, $K = -\frac{1}{2\pi\phi^2}(\log r + K_0(\phi r))$
2nd+3rd	$(\Delta^2 - \tau^2\Delta^3)K = \delta$	n=1, $K = \frac{1}{2}(\tau^2 r + \frac{r^3}{6} + \tau^3 e^{-\frac{r}{\tau}})$
		n=2, $K = \frac{1}{2\pi}(\tau^2 \log r + \frac{r^2}{4} \log r + \tau^2 K_0(\frac{r}{\tau}))$
		n=3, $K = \frac{\tau^2}{4\pi r}(-1 - \frac{r^2}{2\tau^2} + e^{-\frac{r}{\tau}})$
1st+2nd +3rd	$(-\phi^2\Delta + \Delta^2 - \tau^2\Delta^3)K = \delta$	n=1, $K = \frac{1}{2\phi^2}(-r + \frac{C_1 e^{-\sqrt{v}r}}{\sqrt{v}} - \frac{C_2 e^{-\sqrt{w}r}}{\sqrt{w}})$
		n=2, $K = \frac{1}{2\pi\phi^2}(-\log r + C_1 K_0(\sqrt{v}r) - C_2 K_0(\sqrt{w}r))$
		n=3, $K = \frac{1}{4\pi\phi^2 r}(1 + C_1 e^{-\sqrt{v}r} - C_2 e^{-\sqrt{w}r})$
1st+3rd	$(\Delta + \tau^2\Delta^3)K = \delta$	n=1, $K = -\frac{1}{2}(r + \frac{\sqrt{\tau}}{\sqrt{2}} e^{-\frac{r}{\sqrt{2\tau}}} (\cos(\frac{r}{\sqrt{2\tau}}) - \sin(\frac{r}{\sqrt{2\tau}})))$
		n=2, $K = -\frac{1}{2\pi}(\log r + \frac{1}{2}(K_0(r\sqrt{-\frac{i}{\tau}}) + K_0(r\sqrt{\frac{i}{\tau}})))$
		n=3, $K = \frac{1}{4\pi r}(1 - e^{-\frac{r}{\sqrt{2\tau}}} \cos(\frac{r}{\sqrt{2\tau}}))$
2nd+4th	$(\Delta^2 + \tau^2\Delta^4)K = \delta$	n=1, $K = \frac{r^3}{12} - \frac{\tau\sqrt{\tau}}{2\sqrt{2}} e^{-\frac{r}{\sqrt{2\tau}}} (\cos(\frac{r}{\sqrt{2\tau}}) + \sin(\frac{r}{\sqrt{2\tau}}))$
		n=2, $K = \frac{1}{2\pi}(\frac{r^2}{4} \log r + \frac{\tau i}{2}(K_0(r\sqrt{-\frac{i}{\tau}}) - K_0(r\sqrt{\frac{i}{\tau}})))$
		n=3, $K = -\frac{1}{4\pi r}(\frac{r^2}{2} + \tau e^{-\frac{r}{\sqrt{2\tau}}} \sin(\frac{r}{\sqrt{2\tau}}))$

where

$$v = \frac{1 + \sqrt{1 - 4\tau^2\phi^2}}{2\tau^2}, \quad w = \frac{1 - \sqrt{1 - 4\tau^2\phi^2}}{2\tau^2}, \quad C_1 = \frac{w}{v - w}, \quad C_2 = \frac{v}{v - w}$$

## B Fundamental Solutions of the m-Laplacian

The following expression can be found in [3] (pp.496) for  $2m - n > 0$ :

$$K_{m,n} = \mathcal{F}^{-1}(q^{-2m}) = \begin{cases} \frac{(-1)^{\frac{n}{2}+m+1}}{2^{2m-1}\pi^{\frac{n}{2}}(m-1)!(m-\frac{n}{2})!} r^{2m-n} \log r, & n \text{ even} \\ \frac{\Gamma(\frac{n}{2}-m)}{2^{2m}\pi^{\frac{n}{2}}(m-1)!} r^{2m-n}, & n \text{ odd} \end{cases} \quad (18)$$

## C Fourier Transform of Quadratic Forms

We have [4] an expression  $\mathcal{F}(c^2 + P)^\lambda$  for the Fourier transform related to quadratic forms described by  $P$ . We can easily derive from that, the inverse Fourier transform:

$$\mathcal{F}^{-1}[(c^2 + P)^\lambda] = \left(\frac{1}{2\pi}\right)^n \frac{2^{\lambda+1}(\sqrt{2\pi})^n c^{\frac{n}{2}+\lambda}}{\Gamma(-\lambda)\sqrt{\Delta}} \left(\frac{K_{\frac{n}{2}+\lambda}(cQ^{\frac{1}{2}})}{Q^{\frac{1}{2}(\frac{1}{2}n+\lambda)}}\right) \quad (19)$$

where  $c$  is a constant and  $Q$  is the adjoint quadratic form to  $P$  and  $\Delta$  is the determinant of the matrix of coefficients of  $P$ .

The bessel functions of the second kind reduce to expressions involving the exponential if they are half integer order ([8] pp.10)

$$\begin{aligned} K_{n+\frac{1}{2}}(z) &= (-1)^n \left(\frac{\pi}{2z}\right)^{\frac{1}{2}} z^{n+1} \left(\frac{d}{z dz}\right)^n \left(\frac{e^{-z}}{z}\right) \\ &= \left(\frac{\pi}{2z}\right)^{\frac{1}{2}} e^{-z} \sum_{m=0}^n (2z)^{-m} \frac{\Gamma(n+m+1)}{m!\Gamma(n+1-m)} \end{aligned} \quad (20)$$

We will also make use of the fact that  $K_n(z) = K_{-n}(z)$ .

## D Derivations kernel functions of other members of $L^{m,l,s}$ spline family

For the vector splines in 3D we will need the (scalar) kernel associated with the PDE  $(-\Delta + \tau^2 \Delta^3)K = \delta$ . Thus we need to find the inverse Fourier transform of  $\frac{1}{q^2 + \tau^2 q^6}$ . We proceed as section 2.1:

$$\begin{aligned} \frac{1}{q^2 + \tau^2 q^6} &= \frac{1}{q^2} + \frac{-q^2}{\frac{1}{\tau^2} + q^4} \\ &= \frac{1}{q^2} - \frac{1}{2} \left( \frac{1}{q^2 + \frac{i}{\tau}} + \frac{1}{q^2 - \frac{i}{\tau}} \right) \end{aligned} \quad (21)$$

We are primarily interested in the 3D result, but again we list the low dimensional kernels:

- for  $n = 1$  we have:

$$K = \frac{-r}{2} - \frac{\sqrt{\tau}}{2\sqrt{2}} e^{-\frac{r}{\sqrt{2\tau}}} \left( \cos\left(\frac{r}{\sqrt{2\tau}}\right) - \sin\left(\frac{r}{\sqrt{2\tau}}\right) \right)$$

- for  $n = 2$  we have:

$$K = \frac{-1}{2\pi}(\log r + \frac{1}{2}(K_0(r\sqrt{\frac{-i}{\tau}}) + K_0(r\sqrt{\frac{i}{\tau}})))$$

- for  $n = 3$  we have:

$$K = \frac{1}{4\pi r}(1 - e^{-\frac{r}{\sqrt{2}\tau}} \cos(\frac{r}{\sqrt{2}\tau}))$$

For the vector splines in 3D we will also need the (scalar) kernel associated with the PDE  $(\Delta^2 - \tau^2\Delta^4)K = \delta$ . Thus we need to find the inverse Fourier transform of  $\frac{1}{q^4 + \tau^2q^8}$ . We proceed as section 2.1:

$$\begin{aligned} \frac{1}{q^4 + \tau^2q^8} &= \frac{1}{q^4} + \frac{-1}{\frac{1}{\tau^2} + q^4} \\ &= \frac{1}{q^4} + \frac{i\tau}{2} \left( \frac{-1}{q^2 + \frac{i}{\tau}} + \frac{1}{q^2 - \frac{i}{\tau}} \right) \end{aligned} \quad (22)$$

We are primarily interested in the 3D result, but again we list the low dimensional kernels:

- for  $n = 1$  we have:

$$K = \frac{r^3}{12} - \frac{\tau\sqrt{\tau}}{2\sqrt{2}}e^{-\frac{r}{\sqrt{2}\tau}}(\cos(\frac{r}{\sqrt{2}\tau}) + \sin(\frac{r}{\sqrt{2}\tau}))$$

- for  $n = 2$  we have:

$$K = \frac{1}{2\pi}(\frac{r^2}{4}\log r + \frac{\tau i}{2}(K_0(r\sqrt{\frac{-i}{\tau}}) - K_0(r\sqrt{\frac{i}{\tau}})))$$

- for  $n = 3$  we have:

$$K = \frac{-1}{4\pi r}(\frac{r^2}{2} + \tau e^{-\frac{r}{\sqrt{2}\tau}} \sin(\frac{r}{\sqrt{2}\tau}))$$

## References

- [1] A. Le Mehaute and A. Bouhamidi.  $L^{m,l,s}$ -splines in  $R^d$ . *Numerical Methods of Approximation Theory*. D. Braess and L. L. Schumaker (eds.), 9:135–154, 1992.
- [2] L. Mitas and H. Mitasova. General variational approach to the interpolation problem. *Comput. Math. Applic.*, 16(12):983–992, 1988.
- [3] G. Wahba. *Multivariate model building*. In P-J Laurent, A. Le Me'haute, and L. L. Schumaker, Curves and Surfaces. Academic Press, New York, 1991.



- [4] I. M. Gel'Fand and G. E. Shilov. *Generalized functions*. volume 1 Properties and Operations. Academic Press, New York, 1964.
- [5] J. Duchon. Splines minimizing rotation-invariant seminorms in sobolev spaces. *Constructive theory of functions of several variables, Lecture Notes in Mathematics*, 571:85–100, 1977.
- [6] Milton Abramowitz and Irene A. Stegun. *Handbook of mathematical functions*. Dover publications, INC., New York, 1964.
- [7] C. Gu. Rkpack and its applications: Fitting smoothing spline models. *Technical Report 857, University of Wisconsin-Madison.*, May 1989.
- [8] F. Oberhettinger A. Erdelyi, W. Magnus and F. G. Tricomi. *Bateman Manuscript Project (Volumn 2). Higher transcendental functions*. McGraw-Hill, New York, 1953-55.